


Modified time-delay interferometry with an optical frequency comb

Yu-Jie Tan^{✉,*}, Ming-Yang Xu, Pan-Pan Wang[✉], Han-Zhong Wu, and Cheng-Gang Shao^{✉,†}
MOE Key Laboratory of Fundamental Physical Quantities Measurement and Hubei Key Laboratory of Gravitation and Quantum Physics, PGMF and School of Physics, Huazhong University of Science and Technology, Wuhan 430074, People's Republic of China

 (Received 16 June 2022; accepted 22 July 2022; published 3 August 2022)

Both the fluctuations of the onboard lasers and clocks in a space-based gravitational wave interferometer can significantly decrease the sensitivity of the detector to an unacceptable performance level. Implementing a self-referenced optical frequency comb (OFC) driven by the onboard laser can establish the relationship between these two phase fluctuations. This makes a modification of the time-delay interferometry (TDI) combinations, which is originally used to reduce the larger laser phase noise, to simultaneously reduce the phase noises of the onboard lasers and clocks. At present, only a few typically modified combinations with an OFC have been constructed. In this work, we develop a general method obtaining all of the modified TDI combinations, the core of which is a skillful substitution of the time-delay operator. More specifically, with a skillful substitution, one can directly derive the modified TDI combination from an arbitrary TDI combination. This method avoids studying how to reconstruct the modified TDI combination with an OFC.

DOI: [10.1103/PhysRevD.106.044010](https://doi.org/10.1103/PhysRevD.106.044010)

I. INTRODUCTION

The direct observation of gravitational waves (GWs) is of great significance to astronomy and cosmology [1]. Many organizations are actively preparing various types of GW detection plans [2–11]. A GW signal has been first successfully detected by the ground-based detector Advanced Laser Interferometer Gravitational Wave Observatory (LIGO) [12], and then more GW events have been observed [13–15]. Even so, space-based GW detection corresponds to rich wave sources and can open a new window in the low-frequency band, such as 0.1 mHz–1 Hz, that cannot be detected by the ground-based detector, which is expected to provide key information for the basic physics related to early cosmic evolution processes.

A typical space-based GW detector, such as the Laser Interferometer Space Antenna (LISA) [7], consists of three spacecraft separated by long distances, and each spacecraft is equipped with two optical benches (OBs) fixed on the spacecraft platform and two test masses flying in drag-free orbits. The GW signal is expected to be extracted from the change in separation between the adjacent spacecraft measured by heterodyne laser interferometry. In this process, the test-mass acceleration noise and the laser shot noise constitute the instrumental noise floor, which determines the sensitivity limit of the detector. Experimentalists

are also committed to achieving this experimental level. To avoid getting a false signal, the errors and noises exceeding the instrumental noise floor should be reduced by improving the experimental technology, perfecting the theoretical model, or developing good data processing methods. Here, we focus on studying data processing methods to reduce noise.

The laser phase noise is the dominant noise source in the onboard measurements for a typically space-based GW detector. For the heterodyne one-way measurement between any two spacecraft, the laser noise is about 6–11 orders of magnitude larger than the GW signal in the target frequency band [16–18]. Usually, the separations between the spacecraft change over time due to the orbit dynamics, leading to that different arms of the interferometer cannot be maintained as an equal distance. This greatly affects the differential effect of laser noise as well as the similar noises in the experimental system. To achieve the required experimental sensitivity, time-delay interferometry (TDI) is proposed to cancel the laser noise [19] and has also been developed in the matrix representation recently [20]. In essence, as a data postprocessing technique, TDI is to construct a virtual interferometer with equal arm lengths by making the detection data streams time shifted and then synthesized, so as to realize an excellent differential performance of the noises.

In recent years, the TDI technique is further extended to also remove the second-largest noise source, the fluctuations of the onboard clocks. Generally speaking, there are two strategies: One is the ultrastable oscillator (USO) noise

* yjtan@hust.edu.cn

† cgshao@hust.edu.cn

calibrated [21–25], and the other is the optical frequency comb (OFC) system connected [26,27]. For the first strategy, the laser beams are sideband modulated to generate additional interspacecraft measurements, which allow one to remove the USO noises from the data streams processed by the TDI combinations aiming at removing the laser noise, while the GW signals are preserved in the resulting USO-calibrated data. In the previous work [25], we have made an effort to develop a more generalized USO calibration algorithm. For this strategy, an electro-optic modulator (EOM) is used to modulate the clock noise to the laser phase, and then the clock noise is transmitted with the laser between the spacecraft. As the power of the laser diminishes considerably when they travel millions of kilometers between spacecraft, a high-power outgoing laser, such as watt level, is needed. However, it is not easy to directly handle such high laser power for a commercial EOM. Alternatively, one can also make an EOM to modulate a low-power laser, and the power amplifier is designed after the EOM, while the phase fidelity between the carrier and the sideband should be maintained to precisely preserve the information of the laser and clock noises. Both of these are challenging technical developments. For the second strategy, a self-referenced OFC driven by the onboard laser is used to coherently link the fluctuations of the laser and clock, and then one can simultaneously remove the laser and clock noises by modifying the TDI combination. This strategy does not require a phase modulator to generate sidebands to measure the clock noise. The onboard OFC technique has great potential in a space-based GW detection mission, since it can simplify the onboard interferometry system in some degrees; what is more, the space operation of frequency combs has been reported recently [28], showing that the comb system is gradually approaching the requirements of future space missions. Although the equipment size and weight and the power consumption shall be carefully designed, which is greatly challenging in fact, the microcombs being found in a number of applications [29] could be able to offer a solution to this problem. For the innovative OFC TDI scheme [26], it is equivalent to search the modified TDI combination to remove the transfer function-modified laser noise. Currently, a few typically modified TDI combinations with an OFC have been constructed. In this work, we will study how to develop a more general method to derive the modified TDI combinations with an OFC.

The remainder of the paper is organized as follows. In Sec. II, we simply review the general measured data streams for GW detection, as well as the USO-calibrated TDI technique eliminating the laser and clock phase noises. In Sec. III, we introduce the OFC system, based on which the measured data streams are simplified; furthermore, we discover a skillful substitution of the time-delay operators, based on which a general method is

developed to derive the modified TDI combinations with an OFC system. In addition, we take the modified second-generation TDI combinations as an example to present the analysis. The concluding remarks are given in the last section.

II. GENERAL MEASURED DATA STREAMS AND NOISE ELIMINATION FOR GW DETECTION

The notations and conventions follow the definition for the LISA array in Ref. [30]. As shown in Fig. 1, the three spacecraft are labeled 1, 2, and 3, and each spacecraft carries two OBs labeled with primed or unprimed indices, depending on whether the received laser beam is propagating clockwise or counterclockwise around the LISA triangle as seen from above the plane of the constellation. The optical paths between two adjacent satellites are denoted by L_i and $L_{i'}$, and the index i corresponds to the opposite spacecraft. $L_1 \rightarrow L_3 \rightarrow L_2$ ($L_{1'} \rightarrow L_{2'} \rightarrow L_{3'}$) forms a counterclockwise (clockwise) circulation. The unit vectors \vec{n}_i and $\vec{n}_{i'}$ represent the propagating directions of the laser beams in the counterclockwise and clockwise fashion, respectively. To express the time-delayed data streams, the six time-delay operators \mathcal{D}_i and $\mathcal{D}_{i'}$ with $i = 1, 2, 3$ and $i' = 1', 2', 3'$ are introduced, which act on any function $f(t)$ as

$$\begin{aligned} \mathcal{D}_j f(t) &\equiv f(t)_{:j} = f(t - L_j(t)), \\ \mathcal{D}_k \mathcal{D}_j f(t) &\equiv f(t)_{:jk} = \mathcal{D}_k f(t - L_j(t)) \\ &= f(t - L_k(t) - L_j(t - L_k(t))), \end{aligned} \quad (1)$$

where the indices j and k can take the values $1, 2, 3, 1', 2', 3'$ and the speed of light follows the convention $c = 1$.

In general, four measurements are performed per OB: the interspacecraft carrier-to-carrier heterodyne measurement s_i^c , recording the information of the passing GW by measuring the beat note of the incoming light from the

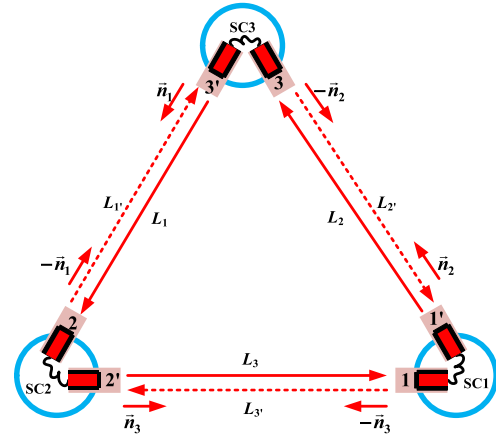


FIG. 1. Notation of the lasers and links in LISA.

distant spacecraft and a local oscillator from the OB; the proof mass-to-OB metrology measurement ε_i , reading out the test mass motion by measuring the beat note of the local oscillator reflected off the test mass and another local oscillator from the adjacent OB; the bench-to-bench metrology measurement τ_i , measuring only the beat note of the two local oscillators, not involving the test mass; the interspacecraft sideband-to-sideband heterodyne measurement s_i^{sb} , achieved by modulating the laser beams exchanged by the spacecraft and comparing the sidebands of the received beam against those of the transmitted beam, which can be used to calibrate out the USO phase fluctuations from the TDI combinations. For the real measurements, the data need to be digitized in an analog-digital converter triggered from the USO (see Fig. 2). As the USO itself is noisy, clock noise is introduced in the sampling process. Alternatively, this measurement can be realized by adopting an OFC system to relate the clock noise to the laser noise. Therefore, the measured data are contributed by the GW signal and also some noises. This paper mainly involves the

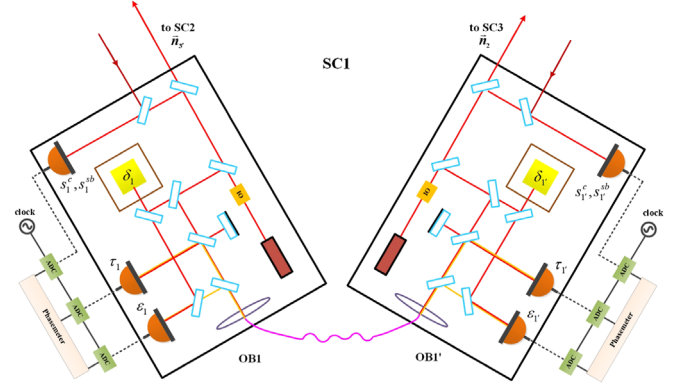


FIG. 2. Schematic diagram of the proof masses and OBs in spacecraft 1.

laser noise, clock noise, OB displacement noise, the test-mass displacement noise, and the laser shot noise. In the USO adopted case, the phase measurements in spacecraft 1, shown in Fig. 2, can be written as the following form [25]:

$$\begin{aligned}
 s_1^c &= H_1 + \mathcal{D}_3 p_{2'} - p_1 + 2\pi\nu_{2'}(\vec{n}_3 \cdot \mathcal{D}_3 \vec{\Delta}_{2'} + \vec{n}_{3'} \cdot \vec{\Delta}_1) + N_1 - a_1 q_1, \\
 s_1^{sb} &= H_1 + \mathcal{D}_3 p_{2'} - p_1 + 2\pi\nu_{2'}(\vec{n}_3 \cdot \mathcal{D}_3 \vec{\Delta}_{2'} + \vec{n}_{3'} \cdot \vec{\Delta}_1) + N_1 + m_2 \mathcal{D}_3 q_2 - m_1 q_1 - c_1 q_1, \\
 \varepsilon_1 &= p_{1'} - p_1 - 4\pi\nu_{1'}(\vec{n}_{3'} \cdot \vec{\delta}_1 - \vec{n}_{3'} \cdot \vec{\Delta}_1) + \mu_{1'} - b_1 q_1, \\
 \tau_1 &= p_{1'} - p_1 + \mu_{1'} - b_1 q_1
 \end{aligned} \tag{2}$$

and

$$\begin{aligned}
 s_{1'}^c &= H_{1'} + \mathcal{D}_{2'} p_3 - p_{1'} + 2\pi\nu_3(\vec{n}_2 \cdot \vec{\Delta}_{1'} + \vec{n}_{2'} \cdot \mathcal{D}_{2'} \vec{\Delta}_3) + N_{1'} - a_{1'} q_1, \\
 s_{1'}^{sb} &= H_{1'} + \mathcal{D}_{2'} p_3 - p_{1'} + 2\pi\nu_3(\vec{n}_2 \cdot \vec{\Delta}_{1'} + \vec{n}_{2'} \cdot \mathcal{D}_{2'} \vec{\Delta}_3) + N_{1'} + m_3 \mathcal{D}_{2'} q_3 - m_{1'} q_1 - c_{1'} q_1, \\
 \varepsilon_{1'} &= p_1 - p_{1'} - 4\pi\nu_1(\vec{n}_2 \cdot \vec{\delta}_{1'} - \vec{n}_2 \cdot \Delta_{1'}) + \mu_1 - b_{1'} q_1, \\
 \tau_{1'} &= p_1 - p_{1'} + \mu_1 - b_{1'} q_1.
 \end{aligned} \tag{3}$$

Here, H_1 and $H_{1'}$ are the GW signal, p_1 and $p_{1'}$, respectively, represent the phase noises of the lasers in 1 and 1' OBs [note that, due to the Doppler effect in the interspacecraft beat note frequency, a scaling factor should be introduced to the time-delay operator to match the TDI algorithms for the interferometric measurements expressed in units of frequency and phase; therefore, when the TDI variables are expressed in unit of frequency, all the time-delay operators should be replaced by $(1 - \dot{L}_i)\mathcal{D}_i$, and the detailed discussion can be seen in Ref. [31]], $\vec{\Delta}_i$ and $\vec{\Delta}_{i'}$ correspond to the displacement noises of the i and i' OBs, and $\vec{\delta}_i$ and $\vec{\delta}_{i'}$ are associated

with the mechanical vibrations of test masses with respect to the local inertial reference frame. N_1 and $N_{1'}$ represent the laser shot noises. As the shot noise is inversely proportional to the laser intensity, we omit its effect in streams ε_1 , $\varepsilon_{1'}$, τ_1 , and $\tau_{1'}$ which describe the beat notes between two local oscillators with strong laser intensities. μ_1 and $\mu_{1'}$ are the noises introduced by the optical fibers linking the two OBs in one spacecraft and have been assumed to be independent of the propagating direction of the laser beams within them. q_i is the clock noise in phase, and the coefficients a_1 , $a_{1'}$, b_1 , $b_{1'}$, c_1 , and $c_{1'}$ can be expressed as the below form:

$$\begin{aligned}
a_1 &= \frac{\nu_{2'}(1 - \dot{L}_3) - \nu_1}{f_1}, \\
a_{1'} &= \frac{\nu_3(1 - \dot{L}_{2'}) - \nu_{1'}}{f_1}, \\
b_1 &= \frac{\nu_{1'} - \nu_1}{f_1}, \\
b_{1'} &= \frac{\nu_1 - \nu_{1'}}{f_1} = -b_1, \\
c_1 &= \frac{(\nu_{2'} + m_2 f_2)(1 - \dot{L}_3) - (\nu_1 + m_1 f_1)}{f_1}, \\
c_{1'} &= \frac{(\nu_3 + m_3 f_3)(1 - \dot{L}_{2'}) - (\nu_{1'} + m_{1'} f_1)}{f_1}, \quad (4)
\end{aligned}$$

$$\begin{aligned}
\eta_i &\equiv s_i^c - \frac{\nu_{(i+1)'}}{\nu_i} \frac{\varepsilon_i - \tau_i}{2} - \frac{\nu_{(i+1)'}}{\nu_{i+1}} \mathcal{D}_{i-1} \frac{\varepsilon_{(i+1)'}}{2} - \frac{\tau_{(i+1)'}}{2} - \mathcal{D}_{i-1} \frac{\tau_{i+1} - \tau_{(i+1)'}}{2} \\
&= H_i + \mathcal{D}_{i-1} p_{i+1} - p_i + 2\pi\nu_{(i+1)'} \vec{n}_{i-1} \cdot [\mathcal{D}_{i-1} \vec{\delta}_{(i+1)'} - \vec{\delta}_i] + N_i + b_{i+1} \mathcal{D}_{i-1} q_{i+1} - a_i q_i, \\
\eta_{i'} &\equiv s_{i'}^c - \frac{\nu_{i-1}}{\nu_i} \frac{\varepsilon_{i'} - \tau_{i'}}{2} - \frac{\nu_{i-1}}{\nu_{(i-1)'}} \mathcal{D}_{(i+1)'} \frac{\varepsilon_{i-1} - \tau_{i-1}}{2} + \frac{\tau_i - \tau_{i'}}{2} \\
&= H_{i'} + \mathcal{D}_{(i+1)'} p_{i-1} - p_i + 2\pi\nu_{i-1} \vec{n}_{i+1} \cdot [\vec{\delta}_{i'} - \mathcal{D}_{(i+1)'} \vec{\delta}_{i-1}] + N_{i'} + (b_{i'} - a_{i'}) q_i \quad (5)
\end{aligned}$$

as well as six synthetic sideband-to-sideband interspacecraft interference data streams:

$$\begin{aligned}
r_i &\equiv \frac{s_i^c - s_i^{sb}}{m_{(i+1)'}} = \frac{f_{i+1}}{f_i} q_i - \mathcal{D}_{i-1} q_{i+1} \approx q_i - \mathcal{D}_{i-1} q_{i+1}, \\
r_{i'} &\equiv \frac{s_{i'}^c - s_{i'}^{sb}}{m_{i-1}} = \frac{f_{i-1}}{f_i} q_i - \mathcal{D}_{(i+1)'} q_{i-1} \approx q_i - \mathcal{D}_{(i+1)'} q_{i-1}. \quad (6)
\end{aligned}$$

Based on these 12 synthetic data streams in Eqs. (5) and (6), the USO-calibrated TDI technique can be fully replicated to eliminate the laser noises and clock noises. Specifically, it combines the six carrier-to-carrier data streams to eliminate the three laser phase noises, and the general form of an arbitrary TDI combination can be expressed as [32]

$$\text{TDI} = \sum_{i=1}^3 (P_i \eta_i + P_{i'} \eta_{i'}), \quad (7)$$

where P_i ($P_{i'}$) is the polynomial of the time-delay operators \mathcal{D}_i and $\mathcal{D}_{i'}$. The instrumental noise floor and GW-signal response of the detector after TDI combinations have been also studied [33–35]. Furthermore, combing the six sideband-to-sideband data streams, one can eliminate the three clock noises. The related analysis can be referred to Refs. [24,25]; we will not go into detail here.

where ν terms represent the frequencies of the laser beams, \dot{L} terms are the ratio of the interspacecraft relative velocities to the light speed, f terms are the frequencies of the USOs, and m terms are integer numbers defining the modulation frequencies. The influences of Doppler motion on these coefficients are extremely small, which will be omitted in this paper. Similarly, one can obtain the streams in the other two spacecraft by cyclic permutation of the indices: $1 \rightarrow 2 \rightarrow 3 \rightarrow 1$.

To eliminate the laser phase noise with primed indices and the OB noises, one can make suitable linear combinations of the data streams and obtain six synthetic carrier-to-carrier interspacecraft interference data streams:

III. MODIFIED TDI IN THE GW DETECTION WITH AN OFC SYSTEM

A. Measured data streams for GW detection with an OFC system

The phase fluctuations of the laser and clock can be linked by using an OFC. As shown in Fig. 3, the local laser and the optical frequency comb are combined at the beam splitter, and the comb laser can be locked to this local laser by adjusting the repetition frequency. Consequently, the radio frequency (rf) reference f_i can be generated by dividing the repetition frequency, which is actually

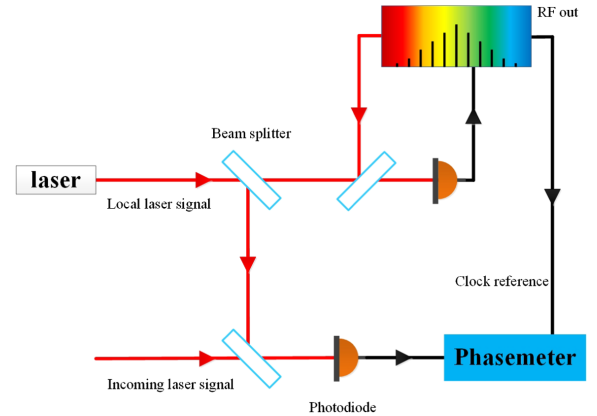


FIG. 3. OFC technique generating a microwave signal coherent to the laser.

traceable to the local laser with a specific down-conversion factor. As a result, the relationship between the clock phase noise $q_i(t)$ and the laser phase noise $p_i(t)$ in the i th spacecraft can be obtained as

$$q_i(t) = \frac{f_i}{\nu_i} p_i(t) + \Delta q_i(t). \quad (8)$$

Since the residual noise $\Delta q_i(t)$ characterizing the coherence level between the laser frequency and the clock frequency has been experimentally demonstrated to be extremely small in the interested frequency band of space-based GW detection [36], this term will be omitted in our analysis. Based on Eq. (8), the 12 synthetic data streams, shown by Eqs. (5) and (6), can be rewritten as

$$\begin{aligned} \eta_i^{\text{OFC}} &= H_i + \mathcal{D}_{i-1} \left(1 + b_{i+1} \frac{f_{i+1}}{\nu_{i+1}} \right) p_{i+1} - \left(1 + a_i \frac{f_i}{\nu_i} \right) p_i \\ &\quad + 2\pi\nu_{(i+1)'} \vec{n}_{i-1} \cdot [\mathcal{D}_{i-1} \vec{\delta}_{(i+1)'} - \vec{\delta}_i] + N_i, \\ \eta_{i'}^{\text{OFC}} &= H_{i'} + \mathcal{D}_{(i+1)'} p_{i-1} - \left[1 + (a_{i'} - b_{i'}) \frac{f_i}{\nu_i} \right] p_i \\ &\quad + 2\pi\nu_{i-1} \vec{n}_{i+1} \cdot [\vec{\delta}_{i'} - \mathcal{D}_{(i+1)'} \vec{\delta}_{i-1}] + N_{i'}, \end{aligned} \quad (9)$$

$$\begin{aligned} r_i^{\text{OFC}} &= \frac{f_i}{\nu_i} p_i - \mathcal{D}_{i-1} \frac{f_{i+1}}{\nu_{i+1}} p_{i+1}, \\ r_{i'}^{\text{OFC}} &= \frac{f_i}{\nu_i} p_i - \mathcal{D}_{(i+1)'} \frac{f_{i-1}}{\nu_{i-1}} p_{i-1}. \end{aligned} \quad (10)$$

$$\begin{aligned} \tilde{\eta}_i &\equiv \rho_i^{-1} \eta_i^{\text{OFC}} = \tilde{\mathcal{D}}_{i-1} p_{i+1} - p_i + \rho_i^{-1} \{ H_i + 2\pi\nu_{(i+1)'} \vec{n}_{i-1} \cdot [K_i \tilde{\mathcal{D}}_{i-1} \vec{\delta}_{(i+1)'} - \vec{\delta}_i] + N_i \}, \\ \tilde{\eta}_{i'} &\equiv K_{i'}^{-1} \eta_{i'}^{\text{OFC}} = \tilde{\mathcal{D}}_{(i+1)'} p_{i-1} - p_i + K_{i'}^{-1} \{ H_{i'} + 2\pi\nu_{i-1} \vec{n}_{i+1} \cdot [\vec{\delta}_{i'} - K_{i'} \tilde{\mathcal{D}}_{(i+1)'} \vec{\delta}_{i-1}] + N_{i'} \}, \end{aligned} \quad (11)$$

where ρ_i , K_i , and $K_{i'}$ are equal to

$$\begin{aligned} \rho_i^{-1} &= \left(1 + a_i \frac{f_i}{\nu_i} \right)^{-1}, \\ K_i^{-1} &= \left(1 + b_{i+1} \frac{f_{i+1}}{\nu_{i+1}} \right) \rho_i^{-1}, \\ K_{i'}^{-1} &= \left[1 + (a_{i'} - b_{i'}) \frac{f_i}{\nu_i} \right]^{-1}, \end{aligned} \quad (12)$$

and the new time-delay operators are expressed as

$$\tilde{\mathcal{D}}_{i-1} \equiv K_i^{-1} \mathcal{D}_{i-1}, \quad \tilde{\mathcal{D}}_{(i+1)'} \equiv K_{i'}^{-1} \mathcal{D}_{(i+1)'}. \quad (13)$$

Since the time-delay operators are time dependent, any pairs of the delay operators do not commute. This means it is impossible to completely eliminate the laser frequency noises by delaying and synthesizing the data streams. In order to use the time-delay technique to make the effective

From Eqs. (9) and (10), all of the clock noises have been effectively converted into laser phase noises in the OFC connected case.

B. Modified TDI combinations with an OFC system

In fact, whether the lasers are operated with sideband modulations or not, six carrier-to-carrier data streams can be obtained and combined to construct the modified TDI combinations to remove both the laser and clock phase noises, i.e., the three effective laser phase noises. At the first sight of the form of Eq. (9), one may naturally think of rewriting the effective laser phase noise terms as the forms of $\mathcal{D}_{i-1} \tilde{p}_{i+1} - \tilde{p}_i$ and $\mathcal{D}_{(i+1)'} \tilde{p}_{i-1} - \tilde{p}_i$, so that the standard TDI combinations capable of eliminating the laser phase noises can be applied directly. However, after some attempts, one may find that this idea is not feasible. As an option, one can also reconstruct the modified TDI combinations in a similar way as searching the standard TDI combinations. In this case, one needs to go through the whole searching process again to reconstruct each modified TDI combination. Here, we consider constructing the forms of the laser phase noise terms as $\tilde{\mathcal{D}}_{i-1} p_{i+1} - p_i$ and $\tilde{\mathcal{D}}_{(i+1)'} p_{i-1} - p_i$; thereby, the standard TDI combinations but replacing \mathcal{D} by $\tilde{\mathcal{D}}$ can be used to eliminate the effective laser phase noises.

Based on Eq. (9), it is convenient to rewrite the heterodyne measurements in the following forms:

laser phase noise, absorbing the clock noises, free to the first order of the velocity of the spacecraft separation, we can substitute Eqs. (11) and (13) into the form of the arbitrary TDI combination in Eq. (7). In this way, one can directly derive the modified TDI combination with an OFC system from an arbitrary TDI combination aiming at standard laser noise suppression. We take the derivation of the modified second-generation TDI combinations as an example to present the process in the following.

The forms of the typical second-generation TDI combinations have been well demonstrated in Refs. [32,37]. For the Michelson combination, we can obtain the modified one as

$$\begin{aligned} \tilde{X}_1^{\text{OFC}} &= [\tilde{\mathcal{D}}_2 \tilde{\mathcal{D}}_2 \tilde{\mathcal{D}}_3 \tilde{\mathcal{D}}_{3'} - I][(\tilde{\eta}_1 + \tilde{\eta}_{2';3}) + (\tilde{\eta}_{1'} + \tilde{\eta}_{3;2'})_{;3'3}] \\ &\quad - [\tilde{\mathcal{D}}_3 \tilde{\mathcal{D}}_3 \tilde{\mathcal{D}}_2 \tilde{\mathcal{D}}_2 - I][(\tilde{\eta}_{1'} + \tilde{\eta}_{3;2'}) + (\tilde{\eta}_1 + \tilde{\eta}_{2';3})_{;22'}] \\ &= K_1^{-2} K_{1'}^{-2} K_{2'}^{-2} K_3^{-2} X_1^{\text{OFC}} \end{aligned} \quad (14)$$

with

$$\begin{aligned} X_1^{\text{OFC}} \equiv & [\mathcal{D}_2 \mathcal{D}_2 \mathcal{D}_3 \mathcal{D}_3 - K_1 K_1' K_2' K_3] [K_1' K_3 (K_1 K_2 \rho_1^{-1} \\ & \times \eta_{1'}^{\text{OFC}} + \eta_{2';3}^{\text{OFC}}) + K_3 (\eta_{1'}^{\text{OFC}} + \rho_3^{-1} \eta_{3;2'}^{\text{OFC}})_{;33}] \\ & - [\mathcal{D}_3 \mathcal{D}_3 \mathcal{D}_2 \mathcal{D}_2 - K_1 K_1' K_2' K_3] [K_1 K_2' K_3 (\eta_{1'}^{\text{OFC}} \\ & + \rho_3^{-1} \eta_{3;2'}^{\text{OFC}}) + (K_1 K_2 \rho_1^{-1} \eta_{1'}^{\text{OFC}} + \eta_{2';3}^{\text{OFC}})_{;22}]. \quad (15) \end{aligned}$$

Here, the effective laser noises, originating from the original laser phase noise and the clock noise, in the data streams have been suppressed free to the first order of the velocity of the spacecraft separation. The clock noises in the synthetic carrier-to-carrier interspacecraft interference data streams shown in Eq. (5) include two parts: One is from the interspacecraft carrier-to-carrier measurements s_i^c and $s_{i'}^c$; the other is from the bench-to-bench measurement $\tau_{i+1} - \tau_{(i+1)'}$ and $\tau_i - \tau_{i'}$, which is introduced to eliminate the laser phase noises with primed indices. If the latter clock noises are neglected, i.e., $K_i^{-1} = \rho_i^{-1}$, Eq. (15) returns to the same result with Eq. (34) in Ref. [26].

Similarly, we can derive the modified Sagnac combination as

$$\begin{aligned} \tilde{\alpha}_1^{\text{OFC}} = & [\tilde{\mathcal{D}}_3 \tilde{\mathcal{D}}_1 \tilde{\mathcal{D}}_2 - I] [\tilde{\eta}_{1'} + \tilde{\eta}_{3';2'} + \tilde{\eta}_{2';1'2'}] \\ & - [\tilde{\mathcal{D}}_2 \tilde{\mathcal{D}}_1 \tilde{\mathcal{D}}_3 - I] [\tilde{\eta}_1 + \tilde{\eta}_{2;3} + \tilde{\eta}_{3;13}] \\ = & K_1^{-1} K_1'^{-1} K_2^{-1} K_2'^{-1} K_3^{-1} K_3'^{-1} \alpha_1^{\text{OFC}} \quad (16) \end{aligned}$$

with

$$\begin{aligned} \alpha_1^{\text{OFC}} = & [\mathcal{D}_3 \mathcal{D}_1 \mathcal{D}_2 - K_1 K_2 K_3] [K_2' K_3 \eta_{1'}^{\text{OFC}} + K_2 \eta_{3';2'}^{\text{OFC}} \\ & + \eta_{2';1'2'}^{\text{OFC}}] - [\mathcal{D}_2 \mathcal{D}_1 \mathcal{D}_3 - K_1' K_2' K_3'] [K_1 K_2 K_3 \\ & \times \rho_1^{-1} \eta_{1'}^{\text{OFC}} + K_2 K_3 \rho_2^{-1} \eta_{2;3}^{\text{OFC}} + K_3 \rho_3^{-1} \eta_{3;13}^{\text{OFC}}], \quad (17) \end{aligned}$$

the modified fully symmetric Sagnac combination as

$$\begin{aligned} \tilde{\zeta}_1^{\text{OFC}} = & [\tilde{\mathcal{D}}_2 \tilde{\mathcal{D}}_3 - \tilde{\mathcal{D}}_1] [\tilde{\eta}_{3;3} - \tilde{\eta}_{3';3} + \tilde{\eta}_{1;1'}] \\ & - [\tilde{\mathcal{D}}_3 \tilde{\mathcal{D}}_2 - \tilde{\mathcal{D}}_1'] [\tilde{\eta}_{1';1} - \tilde{\eta}_{2;2'} + \tilde{\eta}_{2';2'}] \\ = & K_1^{-1} K_1'^{-1} K_2^{-1} K_2'^{-1} K_3^{-1} K_3'^{-1} \zeta_1^{\text{OFC}} \quad (18) \end{aligned}$$

with

$$\begin{aligned} \zeta_1^{\text{OFC}} = & [K_2 \mathcal{D}_2 \mathcal{D}_3 - K_1' K_2' \mathcal{D}_1] (K_1 K_3 \rho_1^{-1} \eta_{1;1'}^{\text{OFC}} - K_3 \eta_{3';3}^{\text{OFC}} \\ & + K_3 K_3' \rho_3^{-1} \eta_{3;3}^{\text{OFC}}) - [K_3' \mathcal{D}_3 \mathcal{D}_2 - K_1 K_3 \mathcal{D}_1'] \\ & \times (K_2 \eta_{1';1}^{\text{OFC}} - K_2 K_2' \rho_2^{-1} \eta_{2;2'}^{\text{OFC}} + K_2 \eta_{2';2'}^{\text{OFC}}), \quad (19) \end{aligned}$$

the modified Relay combination as

$$\begin{aligned} \tilde{U}_1^{\text{OFC}} = & \tilde{\mathcal{D}}_1 [\tilde{\mathcal{D}}_1 \tilde{\mathcal{D}}_3 \tilde{\mathcal{D}}_2 - I] \{\tilde{\eta}_{2'} + \tilde{\eta}_{1';3'} + \tilde{\eta}_{3';2'3'} + \tilde{\eta}_{2;1'2'3'} \\ & - \tilde{\eta}_2\} - [\tilde{\mathcal{D}}_3 \tilde{\mathcal{D}}_2 \tilde{\mathcal{D}}_1 - I] \tilde{\mathcal{D}}_1 \{\tilde{\eta}_{2';1'1} + \tilde{\eta}_{3';1} + \tilde{\eta}_{1';3'1'1}\} \\ = & K_1'^{-2} K_2'^{-2} K_3'^{-2} U_1^{\text{OFC}} \quad (20) \end{aligned}$$

with

$$\begin{aligned} U_1^{\text{OFC}} = & \mathcal{D}_1 [\mathcal{D}_1 \mathcal{D}_3 \mathcal{D}_2 - K_1' K_2' K_3'] [K_1' K_2 K_3 \eta_{2'}^{\text{OFC}} \\ & + K_2 K_3 \eta_{1';3'}^{\text{OFC}} + K_2 \eta_{3';2'3'}^{\text{OFC}} + K_2 \rho_2^{-1} \eta_{2;1'2'3'}^{\text{OFC}} \\ & - K_1' K_2 K_2' K_3' \rho_2^{-1} \eta_2^{\text{OFC}}] - [\mathcal{D}_3 \mathcal{D}_2 \mathcal{D}_1 - K_1' K_2' K_3'] \\ & \times \mathcal{D}_1 [K_1' \eta_{2';1'1}^{\text{OFC}} + K_1' K_2' \eta_{3';1}^{\text{OFC}} + \eta_{1';3'1'1}^{\text{OFC}}], \quad (21) \end{aligned}$$

the modified Beacon combination as

$$\begin{aligned} \tilde{P}_1^{\text{OFC}} = & \tilde{\mathcal{D}}_2 [\tilde{\mathcal{D}}_1 \tilde{\mathcal{D}}_1 - I] \tilde{\mathcal{D}}_3 [\tilde{\eta}_{3';3'} + \tilde{\eta}_{2;1'3'} + \tilde{\eta}_{3;11'3'} - \tilde{\eta}_{3;3'}] \\ & - \tilde{\mathcal{D}}_3' [\tilde{\mathcal{D}}_1 \tilde{\mathcal{D}}_1 - I] \tilde{\mathcal{D}}_2 [\tilde{\eta}_{2;2} + \tilde{\eta}_{3';12} + \tilde{\eta}_{2';1'12} - \tilde{\eta}_{2;2}] \\ = & K_2'^{-2} K_2'^{-2} K_3'^{-2} K_3'^{-2} P_1^{\text{OFC}} \quad (22) \end{aligned}$$

with

$$\begin{aligned} P_1^{\text{OFC}} = & \mathcal{D}_2 [\mathcal{D}_1 \mathcal{D}_1 - K_2 K_3'] \mathcal{D}_3 [K_2 K_3 \eta_{3';3'}^{\text{OFC}} + K_2 K_3 \rho_2^{-1} \\ & \times \eta_{2;1'3'}^{\text{OFC}} + K_3 \rho_3^{-1} \eta_{3;11'3'}^{\text{OFC}} - K_2 K_3 K_3' \rho_3^{-1} \eta_{3;3'}^{\text{OFC}}] \\ & - \mathcal{D}_3' [\mathcal{D}_1 \mathcal{D}_1 - K_2 K_3'] \mathcal{D}_2 [K_2 K_2' K_3' \rho_2^{-1} \eta_{2;2}^{\text{OFC}} \\ & + K_2 \eta_{3';12}^{\text{OFC}} + \eta_{2';1'12}^{\text{OFC}} - K_2 K_3' \eta_{2';2}^{\text{OFC}}], \quad (23) \end{aligned}$$

and the modified Monitor combination as

$$\begin{aligned} \tilde{E}_1^{\text{OFC}} = & \tilde{\mathcal{D}}_3^{-1} [\tilde{\mathcal{D}}_1 \tilde{\mathcal{D}}_1 - I] \tilde{\mathcal{D}}_3 [\tilde{\eta}_{2;3} + \tilde{\eta}_{3';13}] - [\tilde{\mathcal{D}}_1 \tilde{\mathcal{D}}_1 - I] \\ & \times [\tilde{\eta}_{1;11'} - \tilde{\eta}_1] - \tilde{\mathcal{D}}_2^{-1} [\tilde{\mathcal{D}}_1 \tilde{\mathcal{D}}_1 - I] \tilde{\mathcal{D}}_2 [\tilde{\eta}_{3';2'} + \tilde{\eta}_{2;1'2'}] \\ & + [\tilde{\mathcal{D}}_1 \tilde{\mathcal{D}}_1 - I] [\tilde{\eta}_{1';1'1} - \tilde{\eta}_1] \\ = & K_1 K_1' K_2'^{-2} K_3'^{-2} E_1^{\text{OFC}} \quad (24) \end{aligned}$$

with

$$\begin{aligned} E_1^{\text{OFC}} = & K_1' \mathcal{D}_3^{-1} [\mathcal{D}_1 \mathcal{D}_1 - K_2 K_3'] \mathcal{D}_3 [K_2 K_3 \rho_2^{-1} \eta_{2;3}^{\text{OFC}} + \eta_{3';13}^{\text{OFC}}] \\ & - K_1' [\mathcal{D}_1 \mathcal{D}_1 - K_2 K_3'] [K_1 \rho_1^{-1} \eta_{1;11'}^{\text{OFC}} - K_1 K_2 K_3' \rho_1^{-1} \eta_1^{\text{OFC}}] \\ & - K_1 \mathcal{D}_2^{-1} [\mathcal{D}_1 \mathcal{D}_1 - K_2 K_3'] \mathcal{D}_2 [K_2 \eta_{3';2'}^{\text{OFC}} + K_2 \rho_2^{-1} \eta_{2;1'2'}^{\text{OFC}}] \\ & + K_1 [\mathcal{D}_1 \mathcal{D}_1 - K_2 K_3'] [\eta_{1';1'1}^{\text{OFC}} - K_2 K_3' \eta_{1'}^{\text{OFC}}]. \quad (25) \end{aligned}$$

Note all of the time-delay operators in Eqs. (14), (16), (18), (20), (22), and (24) are $\tilde{\mathcal{D}}$, while those in Eqs. (15), (17), (19), (21), (23), and (25) are \mathcal{D} . Equations (17), (19), (21), (23), and (25) are similar to Eqs. (43), (47), (50), (53), and (60) in Ref. [26]. As $a_i, a_{i'}, b_{i+1}, b_{i'} \sim 1$ and $f_i/\nu_i \sim 10^{-8}$ in Eq. (12), the noise floor and the GW response function for the data stream processed with the modified TDI

combinations are nearly the same as those with the standard TDI combinations.

IV. CONCLUSION

The onboard OFC system has great potential to be implemented in a future space-based GW detection mission, since it may simplify the onboard interferometry system. This motivates researchers to study the modified TDI combinations applicable to the noise elimination for GW detection with an OFC. As the OFC technique has linked the laser and clock noises, these modified combinations can simultaneously eliminate these two noises. In this work, based on the characteristics of the synthetic carrier-to-carrier interspacecraft interference data streams, we find that, with a skillful substitution of the time-delay operators, the modified TDI combinations can be directly derived from the standard TDI combinations aiming at laser noise elimination. Furthermore, we take the derivation of the modified second-generation TDI as an example to

present the analysis process. In addition, if the USO system is replaced by the OFC system and all of the lasers are sideband modulated in space-based GW detection, both the six synthetic carrier-to-carrier and six synthetic sideband-to-sideband interspacecraft interference data streams in Eqs. (9) and (10) can be obtained, and one can fully replicate the USO-calibrated TDI technique to eliminate the laser and clock noises. Therefore, the modified TDI combinations and USO-calibrated TDI technique can be combined to mutually check the effectiveness of noise reduction.

ACKNOWLEDGMENTS

This work is supported by the National Natural Science Foundation of China (Grants No. 12175076 and No. 11925503), Guangdong Major Project of Basic and Applied Basic Research (Grant No. 2019B030302001), and the Fundamental Research Funds for the Central Universities, HUST: 2172019kfyRCPY029.

-
- [1] K. S. Thorne, *Gravitational Radiation*, edited by S. W. Hawking and W. Israel (Cambridge University Press, New York, 1987), p. 330.
 - [2] B. Abbott *et al.*, *Rep. Prog. Phys.* **72**, 076901 (2009).
 - [3] J. Aasi *et al.*, *Classical Quant. Grav.* **32**, 074001 (2015).
 - [4] T. Accadia *et al.*, *J. Instrum.* **7**, P03012 (2012).
 - [5] F. Acernese *et al.*, *Classical Quant. Grav.* **32**, 024001 (2015).
 - [6] S. Kawamura *et al.*, *Classical Quant. Grav.* **23**, S125 (2006).
 - [7] P. Amaro-Seoane *et al.*, [arXiv:1702.00786](https://arxiv.org/abs/1702.00786).
 - [8] W. T. Ni, *Int. J. Mod. Phys. D* **22**, 1341004 (2013).
 - [9] B. Hiscock and R. W. Hellings, *Bull. Am. Astron. Soc.* **29**, 1312 (1997).
 - [10] J. Luo *et al.*, *Classical Quant. Grav.* **33**, 035010 (2016).
 - [11] X. Gong *et al.*, *J. Phys. Conf. Ser.* **610**, 012011 (2015).
 - [12] B. P. Abbott *et al.*, *Phys. Rev. Lett.* **116**, 061102 (2016).
 - [13] B. P. Abbott *et al.*, *Phys. Rev. Lett.* **118**, 221101 (2017).
 - [14] B. P. Abbott *et al.*, *Phys. Rev. Lett.* **119**, 161101 (2017).
 - [15] R. Abbott *et al.*, *Phys. Rev. Lett.* **125**, 101102 (2020).
 - [16] M. Tinto and J. W. Armstrong, *Phys. Rev. D* **59**, 102003 (1999).
 - [17] K. McKenzie, R. E. Spero, and D. A. Shaddock, *Phys. Rev. D* **80**, 102003 (2009).
 - [18] LISA Science Study Team, LISA Science Requirements Document, ESA publication, <https://www.cosmos.esa.int/web/lisa/lisa-documents> (2018).
 - [19] M. Tinto and S. V. Dhurandhar, *Living Rev. Relativity* **24**, 1 (2021).
 - [20] M. Tinto, S. V. Dhurandhar, and P. Joshi, *Phys. Rev. D* **104**, 044033 (2021).
 - [21] R. Hellings, G. Giampieri, L. Maleki, M. Tinto, K. Danzmann, J. Hough, and D. Robertson, *Opt. Commun.* **124**, 313 (1996).
 - [22] R. W. Hellings, *Phys. Rev. D* **64**, 022002 (2001).
 - [23] M. Tinto, F. B. Estabrook, and J. W. Armstrong, *Phys. Rev. D* **65**, 082003 (2002).
 - [24] M. Otto, G. Heinzel, and K. Danzmann, *Classical Quant. Grav.* **29**, 205003 (2012).
 - [25] P. P. Wang, Y. J. Tan, W. L. Qian, and C. G. Shao, *Phys. Rev. D* **104**, 082002 (2021).
 - [26] M. Tinto and N. Yu, *Phys. Rev. D* **92**, 042002 (2015).
 - [27] Q. Vinckier, M. Tinto, I. Grudinin, D. Rieländer, and N. Yu, *Phys. Rev. D* **102**, 062002 (2020).
 - [28] B. J. Pröbster, M. Lezius, O. Mandel, C. Braxmaier, and R. Holzwarth, *J. Opt. Soc. Am. B* **38**, 932 (2021).
 - [29] W. Q. Wang, L. R. Wang, and W. F. Zhang, *Advanced Photonics* **2**, 034001 (2020).
 - [30] D. A. Shaddock, M. Tinto, F. B. Estabrook, and J. W. Armstrong, *Phys. Rev. D* **68**, 061303(R) (2003).
 - [31] J. B. Bayle, O. Hartwig, and M. Staab, *Phys. Rev. D* **104**, 023006 (2021).
 - [32] O. Hartwig and J. B. Bayle, *Phys. Rev. D* **103**, 123027 (2021).
 - [33] X. Y. Lu, Y. J. Tan, and C. G. Shao, *Phys. Rev. D* **100**, 044042 (2019).
 - [34] P. P. Wang, Y. J. Tan, W. L. Qian, and C. G. Shao, *Phys. Rev. D* **103**, 063021 (2021).
 - [35] P. P. Wang, Y. J. Tan, W. L. Qian, and C. G. Shao, *Phys. Rev. D* **104**, 023002 (2021).
 - [36] L. S. Ma, Z. Bi, A. Bartels, L. Robertsson, M. Zucco, R. S. Windeler, G. Wilpers, C. Oates, L. Hollberg, and S. A. Diddams, *Science* **303**, 1843 (2004).
 - [37] M. Tinto, F. B. Estabrook, and J. W. Armstrong, *Phys. Rev. D* **69**, 082001 (2004).